

# Motion planning for robot assisted open and MIS pedicle screw insertion surgeries

**Abstract**—Development of robotics and its impact in the medical field has improved efficiency of clinical outcomes, reduced rehabilitation time and made possible, many breakthroughs. Robot assisted pedicle screw insertion , a minimally invasive surgical procedure has proven to be efficient for major spinal fusion and reconstructive surgeries. Increase in domination of technology brings with itself many challenges. Avoidance of collision with efficient path planning in a limited work-space simultaneously ensuring precise accuracy of placement of surgical tools at target anatomy are requirements of the surgery. Although many methods have been tried out for robot assisted surgeries, not many attempts have been tried out for pedicle screw insertion surgery in particular. We propose a new complete motion planning approach that combines an iterative vector based path generation and 3D collision detection algorithm to perform optimal motion planning. The proposed method has been validated in extensive test cases with a 6 DOF robot. The mean relative position error and mean angulation error between planned and actual trajectories were found to be 0.03 mm and 5 respectively.

collision avoidance, path planning, motion planning, robot assisted surgeries, accuracy, pedicle screw

## I. INTRODUCTION

Robot assisted minimally invasive spine surgery procedures have been more successful than conventional surgeries. One of the important procedures in major spine surgeries is placement of the pedicle screw in the vertebrae which has proven to be very effective in spinal reconstructive and stabilization procedures and almost 90% of the spinal fusions surgeries involve this procedure. Conventional open surgeries are subjected to human error and misplacement rates using conventional techniques ranged from 5% to 41% in the lumbar spine and from 3% to 55% in the thoracic spine while placing the pedicle screw and involve more time for rehabilitation. Studies have shown that robot assisted pedicle screw insertion has reduced screw misplacement rates [1] and reduced the risk factors involved and thus have been efficient in improving the accuracy of the pedicle screw placement [2].

Preoperative and intraoperative planning, robotic device systems, and computer-assisted navigation facilitate the placement of pedicle screws by improving the feasibility, accuracy and flexibility of the procedure [3]. Choice of robot, modeling and motion planning of robotic systems also significantly plays a major role in influencing the accuracy re-usability and the level of autonomy of the procedure. Safety is the key factor in robot-assisted surgeries. In order to ensure the success and smooth work of the robot assisted procedure, it is essential to plan the motion of the robot such that it is smooth without any jerk or any abrupt movements and doesn't involve any collision.

Many different approaches of path planning have been tried out for robot-assisted surgeries like venipuncture,orthopaedic surgeries [4], [5]. Various methods have also been tried out for motion planning in dynamic surgical environments [6], [7]. Not many approaches have been tried out specifically for motion planning of robot assisted pedicle screw insertion surgeries. Also, out of all the methods used for surgical motion planning, many were either sampling based or learning based or other grid based techniques [4], [5], [7], [8] giving non-linear paths by either exploring the entire space or based on a heuristic. The pedicle screw insertion points in human vertebrae are spaced in almost orderly fashion which does-not require high sampling or shortest paths.

The following contributions have been made in this paper:

- Motion planning approach combining a novel vector based path planning and 3D collision detection algorithm.
- An extensive validation to evaluate the motion planner in both simulation setup both as well positioning pedicle screws in custom built phantom using a 6 DOF industrial robot(KUKA KR6 R700-2) and image guided system.

This paper is organized as follows: Section 2 describes the path planning and collision detection algorithm used. Section 3 discusses the experimental setup and validation protocol to test the motion planner in simulation and physical robot setup. In Section 4, the results and corresponding analysis. Finally, conclusions are outlined in Section 5.

## II. MATERIALS AND METHODS

### A. Kinematic Analysis of the robot Arm

The movement of a robot arm is realized through the pose of the end effector or variation of angles at each joint of the kinematic chain structure. For a given set of joint angles, the pose of the end-effector of the robot can be obtained from kinematic parameters of a 6 DOF wrist decoupled KUKA manipulator denoted in Modified DH convention as shown in Fig 1. The inverse kinematic method of obtaining joint angle solutions for a given end-effector pose depends on the architecture of the robot arm. Closed form inverse kinematic solutions can be found for robot arms meeting Piper's condition having a wrist decoupled architecture [9]. We have made use of a two step approach to solve inverse kinematics of the robot using an analytical method to solve the 3R spatial structure and euler sequence(ZYX) relation for Wrist decoupled architecture

### B. Motion Planning

Planning the motion of the robot such that there is less or no interaction with the surrounding environment has been the

Joint	$\alpha$	$a_{i-1}$	$d_i$	$\theta$
1	-90	25	400	$\theta_1$
2	0	335	0	$\theta_2$
3	-90	25	0	$\theta_3 - 90$
4	90	0	365	$\theta_4$
5	-90	0	0	$\theta_5$
6	0	0	90	$\theta_6 - 180$

Table I: DH table

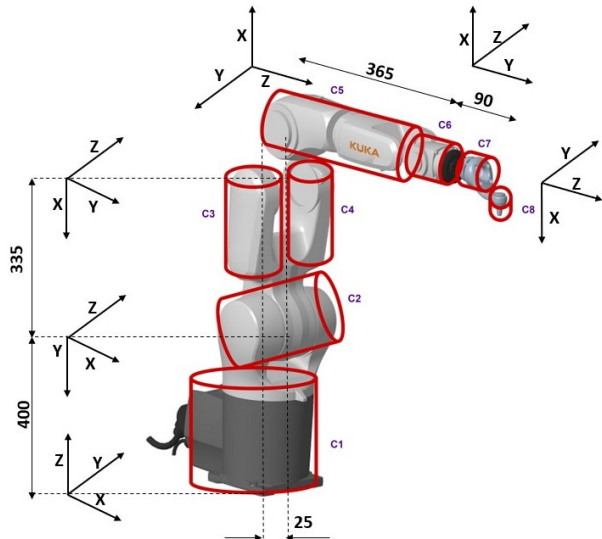


Figure 1: KUKA DH Frame Diagram

topic of research for wide-spread communities for the past few decades. Depending on the use case, constraints and type of robot used, the complexity of the problem statement varies. Joint limits, limited dexterous work space, singularities and requirements of higher order planning according to the degrees of the freedom of the manipulator are constraints of motion planning with serial chain manipulators. Robot assisted pedicle screw insertion surgeries involve very high accuracy and safety of the procedure. It is essential to plan a safe path to reach the target anatomy points in the spine as shown in Fig 2, avoiding all the obstacles: patient, devices and instrument, tools, OT Table. We approach the motion planning problem in modules

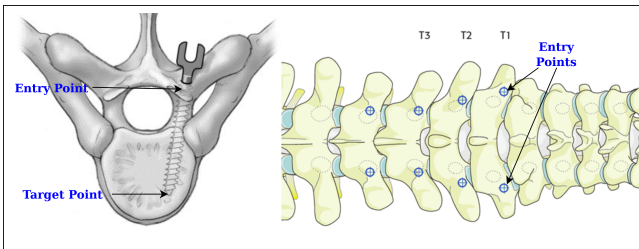


Figure 2: Entry-Target Points

considering all the constraints.

- Algorithm to detect and avoid collision
- 3 Dimensional vector based path planning between given start and goal point
- Orientation profiling of the end-effector tool along the geometrical path

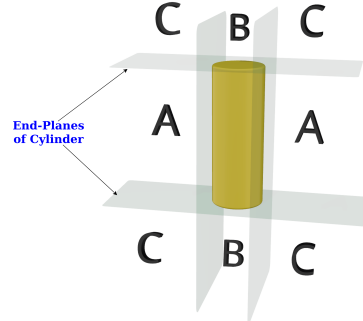


Figure 3: 3D regions around Cylinder

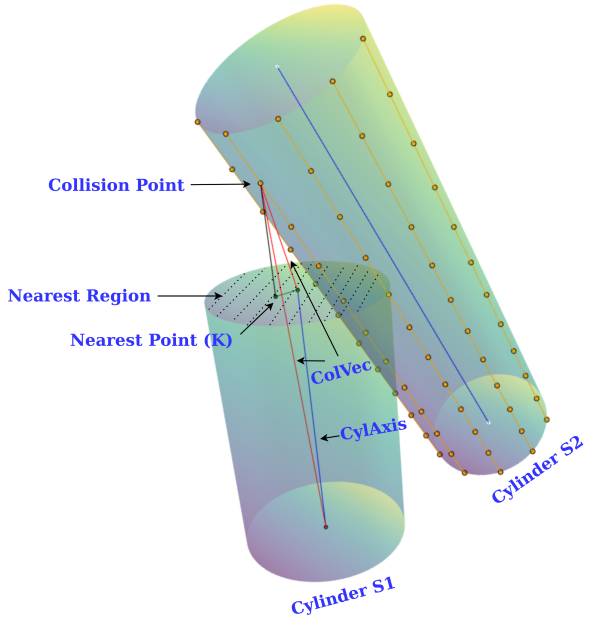


Figure 4: Cylinder- Cylinder Interaction

### C. Collision

In order to ensure safety of a surgical procedure, it is essential to determine the interaction of the robot with its surroundings and avoid interactions that might lead to collision. Assuming very less dynamic changes of the obstacles involved, we have made use of a static collision model focused on obtaining the positional relationship of obstacles with respect to the motion of the robot. Many different approaches have been tried out for modeling obstacles of irregular and regular shapes in a 3D space [10]–[12]. We have used a

geometrical approach to model objects as cylindrical envelopes or plane surface. The shape and structure of tools used in pedicle screw insertion like rods, dilators, reductors and kinematic chain of joints and links of robot arms closely resembles a cylindrical geometry as shown in Fig 1. The flat surface of OT table and patient are considered as plane.

---

**Algorithm 1:** Shortest distance between a point and cylinder

---

```

1 Input
2   Cylinder S1 : Radius, CylPoint1, CylPoint2, CylAxis
3   Cylinder S2 → N line segments → M points
4   3D point(x,y,z) in Approximated Cylinder S2
5    $\alpha \leftarrow 90 - \angle(\text{ColVec2}, \text{CylAxis})$ 
6   RotAxis  $\leftarrow \text{CylAxis} \times \text{ColVec2}$ 
7   A  $\leftarrow \text{RodRot}(\text{ColVec2}, \text{RotAxis}, \alpha)$ 
8 Output
9   PVec : perpendicular vector- nearest region
10  K : shortest point on Cylinder S1 from collision point on
     Cylinder S2
11  Result  $\leftarrow ||\mathbf{K} - \text{point}||_2$ 
12 Case A
13  PVec  $\leftarrow \text{CylAxis}$ 
14  K  $\leftarrow \text{proj}_{\text{PVec}} \text{ColVec2}$ 
15 Case B
16  PVec  $\leftarrow \hat{\mathbf{A}} * \text{Radius}$ 
17  K  $\leftarrow \text{proj}_{\text{PVec}} \text{ColVec2}$ 
18 Case C
19  K  $\leftarrow \hat{\mathbf{A}} * \text{Radius}$ 

```

---

The idea of a cylindrical envelope in 3D space is understood as the intersection of regions contained in between end-planes of the cylinder and cylinder extended to infinity as shown in Fig 3. Intersection between several cylindrical envelopes is used as the base algorithm for collision detection between robot arms and robot and tools. Given two cylindrical envelopes, we approximate the second cylinder as a collection of 'n' number of line-segments as shown in Fig 4. Based on the collective shortest distance of each point on each of line-segments from the first cylinder, we conclude if there is intersection between cylinder S1 and approximated cylinder S2. The shortest distance between a point on S2 from S1 is obtained by finding the point on the nearest region on the cylindrical surface from the point of interest. For points on either sides(case A) and top and bottom of the cylinder(case B), the nearest region is the perpendicular plane cutting through the side of the cylinder and bottom and top plane of cylinders respectively. Instead of considering the entire plane, we have considered the perpendicular vector, namely cylindrical axis vector and vector perpendicular to it respectively. The shortest point(K) is found out by projecting the point on the PVec as mentioned in algorithm 1. For points above and below the end planes and as well as on the sides of the Cylinder (case C) as shown in Fig 3, we find the nearest point by rotating the collision vector onto the top or bottom plane of the cylinder, which will lie on the outer circumference of the top/bottom edge. The obtained shortest distance is used as a measure for path-optimization.

#### D. Path Planning

The limited work-space of the robot covering the spinal region of interest and sequential distribution of entry-target points does not necessitate randomized exploration of the entire 3D space. The focus is directed towards generating an easy to attain geometrical path which can ensure smooth motion as well as easy extension and corrections. The shape of tools used for spinal surgeries also necessitates a proper and smooth geometrical path.

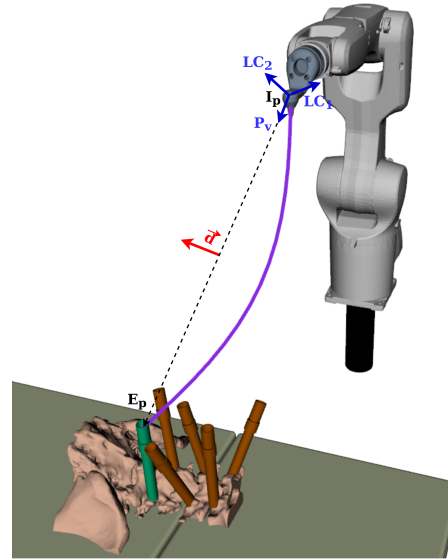


Figure 5: Motion Planner Robot Setup

---

**Algorithm 2:** Path Planning Algorithm

---

```

1 Input
2   Needle Trajectory : EntryPoint Ep, TargetPoint Tp
3   Fixed Home Position for the robot : Ip
4   Ep[3] > Tp[3]
5 Basis Vectors
6   Pv  $\leftarrow E_p - I_p$ 
7   Pp  $\leftarrow [E_p[0], E_p[1], E_p[2]]$ 
8   PLv  $\leftarrow P_p - I_p$ 
9   LC1  $\leftarrow P_v \times PL_v$ 
10  LC2  $\leftarrow LC_1 \times P_v$ 
11  Basis Vectors - Pv, LC1, LC2
12 Algorithm Variability
13  d  $\leftarrow (\hat{P}_v + LC_2 + ||P_v/2||) * \text{Mag-dist}$ 
14  Mag-dist  $\leftarrow (\text{Min-Bound-Value}, \text{Max-Bound-Value})$ 
15  d'  $\leftarrow \text{RodRot}(d, P_v, \theta), \theta \text{ in range}(0, 2\pi)$ 
16 Workflow
17 While(d < Mag-dist):
18   Pathpoints[] = Splinefit(Ip, d', Ep)
19   Col-Stat[] = ColCheck(Pathpoints[])
20   DS-status, Evade-dist = ShortDis(Cyl, Pathpoints)
21   if(paths != NULL) :
22     result  $\leftarrow$  path -greater dead-space distance
23   else:
24     d = d' + Evade-dist

```

---

Unlike the methods used in sampling based or grid based path planning [5], [7], [8], we have chosen a novel vector

based approach to plan the motion of the robot between home position  $I_p$  and entry point of anatomy  $E_p$  as shown in Fig 5. The choice of home position depends on maximum extended height of the robot and other devices in the operating room and the choice of entry/target points depends on specific patient spine anatomical parameters like pedicle angle and diameter of pedicle. We generate spline geometrical paths between these two points.

The shortest path is the straight line  $P_v$ , connecting the Home position  $I_p$  and Entry Point  $E_p$ . We approach the path generation problem by exploring the two perpendicular axes to the straight line  $LC_1$  and  $LC_2$ , thus an orthogonal basis vectors  $LC_1$ ,  $LC_2$  and  $P_v$  as shown in Fig 5. We generate a curve by simultaneously exploring the latitude and longitude vector by maintaining the right ratio between the latitude and longitude vector for which the combination gives a proper curve. We obtain one parameter along the  $P_v$  vector and the other perpendicular to it, namely curvature parameter  $d$ . The flexibility of the algorithm is realized by changing the magnitude and orientation of curvature parameter  $d$ , such that generated spline curves cover the minimum and maximum bounds of workspace covering full circle angulation. Based on the available dexterous work-space of the robot, we decide the MIN-Bound-Value and MAX-Bound-value of variability factor Mag-dist as mentioned in algorithm 2. The curvature of the path ensures natural smoothness as well corrections avoiding sharp turns in case of linear or random paths.

After the path generation, we obtain  $n$  number of paths, we compute the cumulative distance, namely evade-dist as shown in Fig 6, of the path points with respect to the set of already inserted needles for each path based on the shortest distance obtained from cylinder-point interaction mentioned in above section. We then use an elimination approach to filter out those that have the cumulative distance factor less than the minimum dead space requirements as shown in Fig 7. The procedure is repeated by varying the curvature parameter "d" and subsequent "evade-dist", until we find an optimized path away from collision or a sub optimal path as mentioned in algorithm 2.

#### E. Communication Software

The KUKA KR6R700-2 6 DOF industrial robot is equipped with a controller KRC5 Micro, which uses the programming language KRL (KUKA Robot Language) for internal communication. Python was used as the programming language for developing the computational mathematical models and other system integrations. Using the EKI (Ethernet KRL Interface) package, a UDP protocol-based ethernet socket communication that enables the data transfer from python to KRL. A C# based interactive application was developed to plan pedicle trajectories upon CT volume. The application also uses REST API calls to communicate with the IR camera for live tracking and the robot for pedicle placement. The whole software module runs on an i7 Intel processor with 16 GB ram and Nvidia 1060 Ti with 8 GB graphics memory.

### III. EXPERIMENTAL SETUP AND VALIDATION

The proposed path planning, collision detection, path optimization techniques have been extensively validated in a 3D simulation environment. The results obtained in the simulation environment has been verified with physical robot using custom phantom experiment along with system accuracy evaluation.

#### A. Simulation

The important factor associated with pedicle screw insertion in spine surgeries is determining the accuracy of screw placement measured by an anatomical parameter: pedicle angle consisting transverse pedicle angle (TPA) and sagittal pedicle Angle (SPA) [13]. In order to replicate the same scenario of different deformities and conditions where pedicle screw insertion becomes useful, we validate the motion planner by simulating different scenarios by varying the following parameters: SPA, TPA angles are taken as  $(\theta, \alpha)$  defined in spherical coordinate system convention and inter pedicle distance  $d$ . We test the motion planner for a set of 6 to 8 target points in lumbar and thoracic spine phantom as shown in Fig 8. SPA and TSA angles are taken in a range of  $-60^\circ$  to  $60^\circ$  and  $-45^\circ$  to  $45^\circ$  respectively. We sample a set of combination of SPA and TSA with inter pedicle distance of 4.5 to 7.5 mm for thoracic region and 8.5 to 10.5 mm for lumbar region which is super-set of range quoted in medical literature [14], [15].

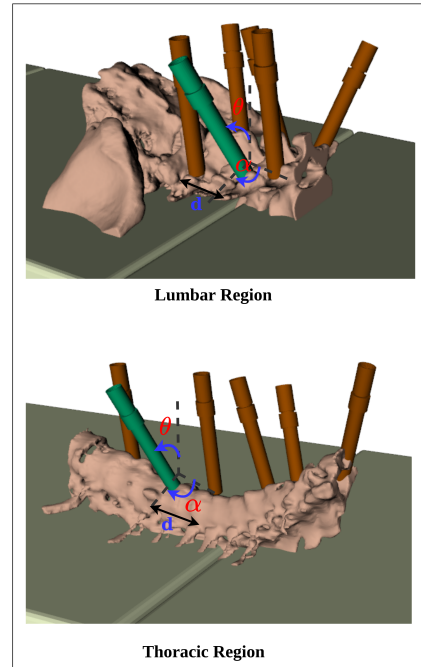


Figure 6: Test cases

The validation test cases are split into 4 divisions, based on the order of pedicle screw insertion. In first division of test cases, we use sequential ordering of plans, where we traverse the right side of anatomy first then followed by left

and vice versa. We can find n different test cases for n target points . This kind of sequencing is primarily used in pedicle screw insertion surgeries and most preferable by doctors. In the second division of test cases, we use simultaneous ordering of plans, where we traverse left and right of each vertebrae one by one. Using permutations, we can find 16-24 test cases for 8 target points. Out of the 24 test cases, some cases might be acceptable by pedicle screw insertion surgical procedure and other test cases due to inherent collision between the plans of left and right colliding. In third division of test cases, we place clusters of pedicles at random order for given inter-pedicle distance and range of pedicle angle and test the feasibility of the next upcoming plan. There can be 24-48 different test cases for 8 target points, out of which some cases might have inherent collision and other test cases which are acceptable by standards of spine surgeries. In fourth division of test cases, we generate a random sample of target points which have uneven distribution of inter pedicle distances and random samples of pedicle angle. The merits of the proposed motion planner is scrutinized in the last set of test cases.

### B. Experimental setup for physical robot validation

We have used a custom designed tool accuracy phantom with delrin material for evaluating the overall system accuracy along with validation of motion planner test cases proposed in simulation and we have used a NDI Polaris IR Camera for tracking the pedicle screw trajectory. We registered the phantom with CT and obtained the coordinates of Entry- Target points in the dicom image. Through Iterative closest point (3 point/ surface) registration we obtained the transformation between the dicom and IR camera and through 3 point ICP registration we obtained the transformation between Robot and IR camera. We used an interactive C# app for visualizing the plans. The phantom consists of a number of screw heads covering a sector of TPA and SPA. The phantom was placed in the suitable dexterous work-space on both left and right side of robot docking and all 4 divisions of test cases evaluated in simulation were validated on both sides of docking taking a suitable region of interest.

A calibrated stainless steel end-effector as shown in Fig 1, with less than 0.2 mm position calibration error was used for experimental analysis. We assumed errors due to joint calibration and mounting were negligible. We have used a calibrated tracking tool with 4 fiducial markers. We positioned the robot in different plans consisting of 17 different sets of pedicle angles covering 4 quadrants in 3D space ,with range of SPA and TPA both varying from -35° to 25° and simultaneously tracked the tool through the camera and viewed the results between planned and actual trajectories in the app. From our observations, we quote the average relative position error and average angulation error. The relative position error is measured by euclidean distance between the planned target point and actual target point viewed in the dicom coordinate system,  $RPE = \|TP_{actual} - TP_{measured}\|$  .The relative angulation error is measured as the angle deviation of planned trajectory wrt actual trajectory, Deviation =  $\angle(Traj_{actual}, Traj_{planned})$ .

Test cases		
SNO.	Type	Success%
1	Sequential	100
2	Simultaneous	98
3	Random sequencing	92
4	Random Sample	88
-	Overall	94.5

Table II: Motion Planner test results

Accurcay Metrics	
Mean RPE(mm)	Mean angle error(°)
0.45	3

Table III: Delrin Phantom Accuracy Metrics

## IV. RESULTS AND DISCUSSION

In this section, we discuss about the results obtained from extensive validation experiment in simulation and physical robot and provide some analysis on failure test cases.

The motion planner was 100 % successful in sequential planning test cases in both simulation as well in physical root evaluation and 98 % successful for simultaneous test cases and didn't produce optimised results for test cases which involved inter pedicle distance less than or equal to 1.5 times the diameter of end-effector. In test cases involving random plans for fixed range of pedicle angles and inter-pedicle distance, the success percentage was 92%. In rest of the test cases, there was plan found for planned pedicle angle which was either already colliding with the adjacent plans or sampled target point has SPA value in opposite with SPA adjacent plan. In complex test cases involving random pedicle angle and inter pedicle range, we observed that the success was 88 %. The motion planner couldn't find optimised paths for cases where inter pedicle region less than end-effector diameter, colliding adjacent pedicle angles and as well as target points sampled in middle of already sampled plans covering pedicle angles which leaves very less clearance place for the given end-effector to position. In general, the trajectory plans in the further left took longer time for right side docking and vice versa for left side docking.

A simple test for evaluating the robot accuracy was performed and through visual inspection. We observed that accuracy value was less than 2 mm for almost all of the cases, less than 1 mm for cases with entry points sampled with pedicle angle 0°-30° and 1-2 mm for range of pedicle angle above 30°. Thus, it can inferred that the accuracy value was in direct proportion to the entry point accuracy, as for the same target point the the value of accuracy decreased as the angle increased. The corresponding pattern of accuracy change was viewed in custom phantom experiments with additional accuracy error due to registration. The overall system accuracy is reported in two metrics: relative position error and angle

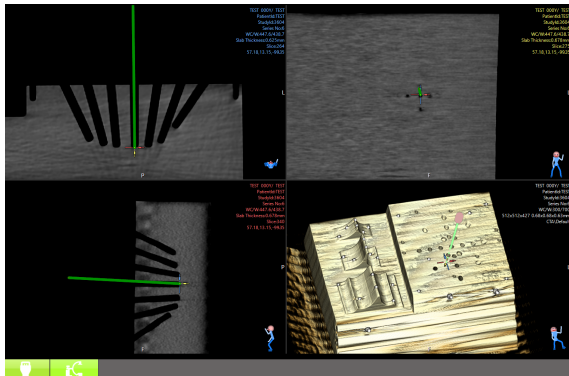


Figure 7

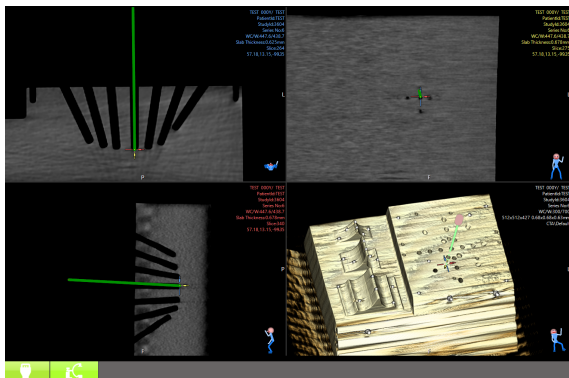


Figure 8: Accuracy Evaluation

error between the planned and actual trajectories. The average relative position error over 17 plans was noted to be ...mm , the maximum error was found to be ... mm and the minimum error was found to be ...mm . The average angle deviation over 17 plans was found to be ..°, the maximum and minimum angulation error were found to be ...°and ...°respectively.

## V. CONCLUSION

The feasibility and effectiveness of the proposed motion planning algorithm has been successfully demonstrated in extensive validation. The simulation and experimental results verified that the proposed method generated optimized path that are away from the collision in 94.5% of the test cases covering the 4 divisions. Further work would involve improving the low computational efficiency of the motion planner due to complete 3D obstacle detection. Further, we also hope to extend this work to include dynamic obstacles in surgical environment and validate in cadaver and clinical trials.

## REFERENCES

- [1] Belmont, Philip J. Jr., MD; Klemme, William R. MD; Dhawan, Aman MD; Polly, David W. Jr., MD In Vivo Accuracy of Thoracic Pedicle Screws, Spine: November 1, 2001 - Volume 26 - Issue 21 - p 2340-2346.
- [2] Li HM, Zhang RJ, Shen CL. Accuracy of Pedicle Screw Placement and Clinical Outcomes of Robot-assisted Technique Versus Conventional Freehand Technique in Spine Surgery From Nine Randomized Controlled Trials: A Meta-analysis. *Spine (Phila Pa 1976)*. 2020 Jan 15;45(2):E111-E119. doi: 10.1097/BRS.0000000000003193. PMID: 31404053.
- [3] Tian, Nai-Feng, and Hua-Zi Xu. "Image-guided pedicle screw insertion accuracy: a meta-analysis." *International orthopaedics* vol. 33,4 (2009): 895-903. doi:10.1007/s00264-009-0792-3.
- [4] F. Li, Z. Huang and L. Xu, "Path Planning of 6-DOF Venipuncture Robot Arm Based on Improved A-star and Collision Detection Algorithms," 2019 IEEE International Conference on Robotics and Biomimetics (RO-BIO), 2019, pp. 2971-2976, doi: 10.1109/ROBIO49542.2019.8961668.
- [5] Nguyen, Q.C., Kim, Y., Park, S. et al. End-effector path planning and collision avoidance for robot-assisted surgery. *Int. J. Precis. Eng. Manuf.* 17, 1703–1709 (2016). <https://doi.org/10.1007/s12541-016-0197-3>.
- [6] Sozzi A, Bonfè M, Farsoni S, De Rossi G, Muradore R. Dynamic Motion Planning for Autonomous Assistive Surgical Robots. *Electronics*. 2019; 8(9):957. <https://doi.org/10.3390/electronics8090957>.
- [7] N. Sayols et al., "Global/local motion planning based on Dynamic Trajectory Reconfiguration and Dynamical Systems for Autonomous Surgical Robots," 2020 IEEE International Conference on Robotics and Automation (ICRA), 2020, pp. 8483-8489, doi: 10.1109/ICRA40945.2020.9197525.
- [8] M. Elbanhawi and M. Simic, "Sampling-Based Robot Motion Planning: A Review," in *IEEE Access*, vol. 2, pp. 56-77, 2014, doi: 10.1109/ACCESS.2014.2302442.
- [9] Seemal Asif, Philip Webb, "Kinematics Analysis of 6-DoF Articulated Robot with Spherical Wrist", *Mathematical Problems in Engineering*, vol. 2021, Article ID 6647035, 11 pages, 2021. <https://doi.org/10.1155/2021/6647035>.
- [10] M. Melchiorre, L. S. Scimmi, S. P. Pastorelli and S. Mauro, "Collision Avoidance using Point Cloud Data Fusion from Multiple Depth Sensors: A Practical Approach," 2019 23rd International Conference on Mechatronics Technology (ICMT), 2019, pp. 1-6, doi: 10.1109/ICMECT.2019.8932143.
- [11] Das, N., Yip, M. C. (2020). Stochastic modeling of distance to collision for robot manipulators. *IEEE Robotics and Automation Letters*, 6(1), 207-214.
- [12] Das, N., Yip, M. (2020). Learning-based proxy collision detection for robot motion planning applications. *IEEE Transactions on Robotics*, 36(4), 1096-1114.
- [13] Osman, N. D., Suhaimi, N. M., Saidun, H. A., Mat, M. A. S. Metal Artefact Reduction with Different Transverse Angles of Metal Placement and Gantry Tilt Angulation in Spine CT Imaging.
- [14] Agrawal, M., Devarajan, L. J., Dharanipathy, S., Katiyar, V., Singh, P. K., Garg, A., ... Kale, S. S. (2021). Morphometric Analysis of C2 Pedicle in 247 Patients and Proposal for Trajectory and Size of Pedicle Screw. *Neurology India*, 69(4), 925.
- [15] Bernard TN Jr, Seibert CE. Pedicle diameter determined by computed tomography. Its relevance to pedicle screw fixation in the lumbar spine. *Spine (Phila Pa 1976)*. 1992 Jun;17(6 Suppl):S160-3. doi: 10.1097/00007632-199206001-00017. PMID: 1385900.